REFINED RECONSTRUCTION TECHNIQUES FOR LDA DATA ANALYSIS

H. Nobach, E. Müller

Universität Rostock, Fachbereich Elektrotechnik
Institut für Nachrichtentechnik und Informationselektronik
Richard-Wagner-Straße 31, 18119 Rostock, Germany

C. Tropea

Lehrstuhl für Strömungsmechanik, Universität Erlangen-Nürnberg
Cauerstraße 4, 91058 Erlangen, Germany

ABSTRACT

A new spectral estimator for LDA data is introduced, based on one-point reconstruction techniques, but employing a refinement which accounts in a statistical manner for the velocity change between a particle arrival and the sample instant. The technique successfully eliminates the low-pass filter behavoir associated with reconstruction techniques in general and is therefore particularly interesting for the estimation of spectra at low data rates. The new estimator is demonstrated using experimental data and simulations. The evaluation is supplemented by comparisons with low-noise, hot-wire data.

1. INTRODUCTION

LDA data analysis, especially spectral estimation, has often been performed using a signal reconstruction, yielding data with equal time spacing between measurements. The statistical properties of such reconstructed data can differ significantly from the those of the physical process being measured. Among other effects, conventional reconstruction techniques introduce a finite correlation time to the originally uncorrelated noise component of the velocity time history, which is equivalent to a low-pass filter. This effect has been well documented for specific reconstruction schemes and is easily observable in measured power spectral densities (Adrian, Yao; 1987). In fact, this appears to be the dominating effect of reconstructed signals, meaning that even among reconstruction schemes, it is often difficult to give a general preference (Müller et al.; 1994).

The present work examines the possibility of improving autocorrelation and spectral estimates from reconstructed signals, using knowledge about the particle arrival statistics to *correct* the raw estimates. The techniques discussed here are applicable only for one-point interpolation schemes, i.e. interpolation between LDA data points irregularly spaced in time, which use only the last valid data point for interpolation within that interval. This would include the widely used *sample and hold interpolation* **(S+H)** (Adrian, Yao; 1987) or the *single exponential interpolation* (Høst-Madsen; 1994). The technique is not suitable for use with a linear interpolation or, for instance, a fractal reconstruction, in which two or more data points are used to interpolate missing intervals of the data set.

As in many previous suggestions for estimating power spectra, the goal is to reduce the effect of noise in LDA data sets as well as the variance of the estimates — goals which are usually compatible with one another [2,10,13,18]. Furthermore, interest lies in achieving these goals also under the constraint of low data rates.

The refined reconstruction technique is introduced in section 2 including details of the solution algorithms. A brief description of the simulation procedure and experiments used to test the technique is given in section 3. The performance of the technique is then studied in section 4 with some conclusions and outlook for further work given in section 5.

2. ESTIMATION PROCEDURE

The estimation of the power spectral density (PSD) function of turbulent velocity fluctuations can be broadly subdivided into *non-parametric* and *parametric* methods, as illustrated in Fig. 1. The present technique is classified as non-parametric and uses as a starting point, existing methods of one-point signal reconstruction, re-sampling and equal time sampled PSD estimators. This PSD estimate is then refined on the basis of knowledge about the mean time between velocity samples and the distribution of the interarrival times. The approach is to derive an expression for the resampled autocorrelation function in terms of the true autocorrelation function, in a manner very similar to that presented by Adrian and Yao (1987). This relation is then inverted to estimate the true autocorrelation function from the measured resampled autocorrelation. The PSD estimate follows using a Fourier transform.

2.1 Expression For Resampled Autocorrelation Function

The derivation begins by examining the time periods involved in LDA data acquisition and resampling, as illustrated in Fig. 2 for the case of a sample and hold reconstruction. There are basically three superimposed processes: 1) the arrival of validated LDA data at the times, $t_{LDA;i}$; 2) the resolution of time measurement in the ac-

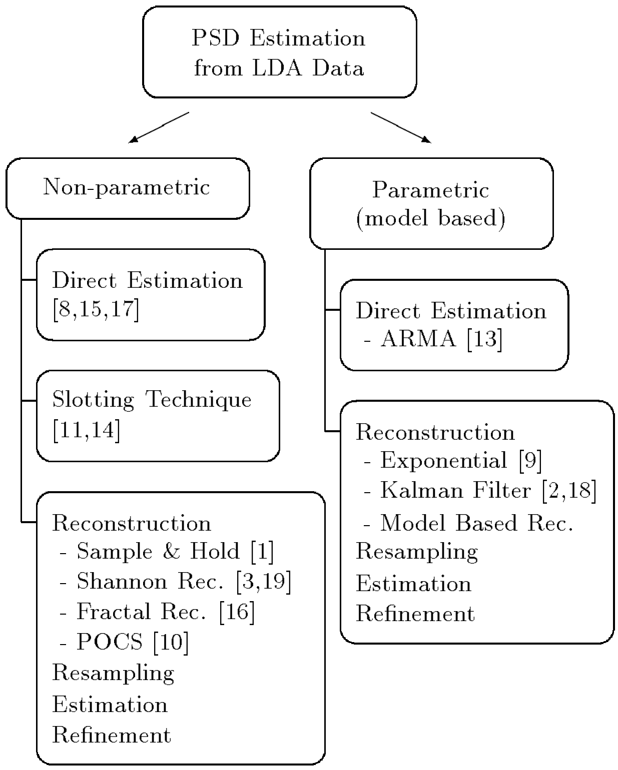

Figure 1: Overview of estimation techniques for power spectral density from LDA Data

Table 1: Possible reconstruction functions. ρ_{model} is the autocorrelation coefficient of the model process.

Reconstruction technique	$f_{rec}(\xi_j - t_i)$
Sample and hold (S+H)	1
Autoregressive 1st order (AR1) (Exponential)	$\phi_1^{\xi_j - t_i}$
Model based reconstruction	$\rho_{model}(\xi_j - t_i)$

quisition system, t_i; 3) and the resample times ξ_j. The resample times are necessarily coincident with the time resolution steps and for present purposes these steps are assumed to be unity ($\xi_j = j$). Furthermore, this primary time resolution is assumed to be so high, that the time difference $t_{LDA;i} - t_i$ is negligible in terms of flow dynamics, i.e. $t_{LDA;i} = t_i$ and $u_{LDA;i} = u(t_i)$. In principle this time resolution will limit the spectral resolution at the high frequency end, however other factors prohibit this limit from being reached, as shown below.

Quite generally the reconstructed velocity signal can be expressed for one-point reconstruction techniques as:

$$u_{rec}(\xi_j) = u_{LDA;i} f_{rec}(\xi_j - t_i) \tag{1}$$

where $t_i - 1 \le t_{LDA;i} < t_i \le \xi_j \le t_{i+1} - 1 \le t_{LDA;i+1} < t_{i+1}$. The function f_{rec} depends on the selected reconstruction method, several possibilities are summarized in Table 1.

The autocorrelation of the reconstructed velocity signal

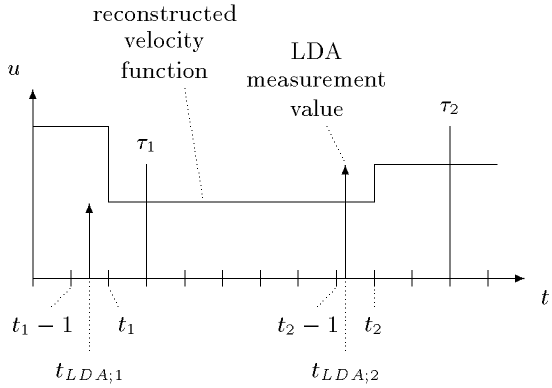

Figure 2: Principle relationship between arrival times and resample times

is given by

$$R_{rec}(\tau_1; \tau_2) = E\{u_{rec}(\tau_1) u_{rec}(\tau_2)\} \tag{2}$$

Assuming stationarity this definition becomes time independent and can be written as

$$R_{rec}(\tau) = E\{u_{rec}(\xi_j) u_{rec}(\xi_j + \tau)\} \tag{3}$$

which can be estimated from a finite data set as

$$\hat{R}_{rec}(\tau) = \frac{1}{N} \sum_{j=1}^{N} u_{rec}(\xi_j) u_{rec}(\xi_j + \tau) \tag{4}$$

where τ is simply the number of primary time steps between resample instances. Before proceeding to evaluate this expression, it is now necessary to examine the statistics of the time periods $\xi_j - t_i$.

The statistics of particle arrivals have been thoroughly studied [4,5] in the past. For a random spatial distribution of the seed particles, the time between particle arrivals is exponentially distributed with an exponent equal to the instantaneous particle rate

$$\dot{n}(t) = cA(\vec{u})|\vec{u}| \tag{5}$$

where c is the volume concentration and $A(\vec{u})$ is the detection area of the measurement volume projected normal to the velocity vector $\vec{u}$.

The probability of no particle arrival in the time interval $[t_i; \xi_j)$ is therefore

$$\begin{aligned} p(n = 0; t_i; \xi_j) &= e^{-\int_{t_i}^{\xi_j} \dot{n}(\tau)\, d\tau} \\ &\approx e^{-\dot{n}(\xi_j - t_i)} \end{aligned} \tag{6}$$

The second expression assumes time invariance of $\dot{n}$ over short intervals. Conversely the probability of receiving at least one particle arrival in the same interval becomes

$$p(n \ge 1; t_i; \xi_j) = 1 - e^{-\dot{n}(\xi_j - t_i)} \tag{7}$$

To now derive an expression for the autocorrelation function of the reconstructed velocity signal in terms of the true autocorrelation function, it is neccessary to examine the velocity values at two times τ_1 and τ_2 and their probability of occurence. Two different situations must be examined.

1. one measurement value at $t_{LDA;1}$ such that $t_1 - 1 \leq t_{LDA;1} < t_1 \leq \tau_1$ no further measurement value between t_1 and τ_1 and one further measurement value such that $\tau_1 \leq t_2 - 1 \leq t_{LDA;2} < t_2 \leq \tau_2$ and no further value in the intervall $[t_2; \tau_2)$. In this case

$$\begin{aligned} u_{rec}(\tau_1) &= u_{LDA;1} f_{rec}(\tau_1 - t_1) \\ u_{rec}(\tau_2) &= u_{LDA;2} f_{rec}(\tau_2 - t_2) \end{aligned} \tag{8}$$

with an occurence probability denoted by p_1.

2. one measurement value at $t_{LDA;1}$ such that $t_1 - 1 \leq t_{LDA;1} < t_1 \leq \tau_1$ and no further measurement value in the interval $[t_1; \tau_2)$. In this case

$$\begin{aligned} u_{rec}(\tau_1) &= u_{LDA;1} f_{rec}(\tau_1 - t_1) \\ u_{rec}(\tau_2) &= u_{LDA;1} f_{rec}(\tau_2 - t_1) \end{aligned} \tag{9}$$

with an occurence probability denoted by p_2.

The probabilities of these two situations are respectively

$$\begin{aligned} p_1 &= (1 - e^{-\dot{n}})^2 e^{-\dot{n}(\tau_1 + \tau_2 - t_1 - t_2)} = p_1(\tau_1; \tau_2; t_1; t_2) \\ p_2 &= (1 - e^{-\dot{n}}) e^{-\dot{n}(\tau_2 - t_1)} = p_2(\tau_1; \tau_2; t_1) \end{aligned} \tag{10}$$

The autocorrelation function given by Eq. (2) can now be written

$$\begin{aligned} R_{rec}(\tau_1; \tau_2) = & \\ & \sum_{t_1=-\infty}^{\tau_1} \sum_{t_2=\tau_1+1}^{\tau_2} E\{u(t_1) f_{rec}(\tau_1 - t_1) u(t_2) f_{rec}(\tau_2 - t_2)\}\, p_1 \\ & + \sum_{t_1=-\infty}^{\tau_1} E\{u(t_1) f_{rec}(\tau_1 - t_1) u(t_1) f_{rec}(\tau_2 - t_1)\}\, p_2 \end{aligned} \tag{11}$$

These equations can be simplified somewhat by setting $\tau_1 = 0$, which assumes an arbitrary reference time of a stationary process.

$$\begin{aligned} p_1' &= p_1'(\tau; t_1, t_2) = p_1(0; \tau; t_1, t_2) \\ &= (1 - e^{-\dot{n}})^2 e^{-\dot{n}(\tau - t_1 - t_2)} \\ p_2' &= p_2'(\tau; t_1) = p_2(0; \tau; t_1) \\ &= (1 - e^{-\dot{n}}) e^{-\dot{n}(\tau - t_1)} \end{aligned} \tag{12}$$

A final expression for the autocorrelation function of the reconstructed velocity signals can now be written

$$\begin{aligned} R_{rec}(\tau) = & \\ & \sum_{t_1=-\infty}^{0} \sum_{t_2=1}^{\tau} E\{u(t_1) f_{rec}(-t_1) u(t_2) f_{rec}(\tau - t_2)\}\, p_1' \\ & + \sum_{t_1=-\infty}^{0} E\{u(t_1) f_{rec}(-t_1) u(t_1) f_{rec}(\tau - t_1)\}\, p_2' \\ = & \sum_{t_1=-\infty}^{0} \sum_{t_2=1}^{\tau} R_{uu}(t_2 - t_1) f_{rec}(-t_1) f_{rec}(\tau - t_2)\, p_1' \\ & + \sum_{t_1=-\infty}^{0} R_{uu}(0) f_{rec}(-t_1) f_{rec}(\tau - t_1)\, p_2' \end{aligned} \tag{13}$$

which is in fact now expressed in terms of the true autocorrelation function $R_{uu}(\tau)$.

This expression has been verified using simulation techniques described briefly in the next section. A velocity time series with known spectrum (autocorrelation function) was generated and used to simulate LDA particle arrivals at a mean data rate of 0.316 and for 10 000 time units. Fig. 3 compares the input spectrum with the spectrum deduced from Eq. (13) (after applying a Fourier transform) and with the estimated spectrum directly from Eq. (4) over the finite sample size for a sample and hold reconstruction. Clearly Eq. (13) describes the autocorrelation function of the reconstructed signal well. Fig. 3b illustrates similar performance using an AR1 reconstruction.

2.2 Refinement Of The Estimate

Using the transformation $\xi = t_2 - t_1$, Eq. (13) can be written as

$$\begin{aligned} R_{rec}(\tau) = & \\ & R_{uu}(0) \sum_{t_1=-\infty}^{0} f_{rec}(-t_1) f_{rec}(\tau - t_1) p_2'(\tau; t_1) \\ & + \sum_{\xi=1}^{\infty} R_{uu}(\xi) \sum_{t_2=1}^{\min(\tau;\xi)} f_{rec}(\xi - t_2) f_{rec}(\tau - t_2) \cdot \\ & \cdot p_1'(\tau; t_2 - \xi; t_2) \end{aligned} \tag{14}$$

which is a linear system of equations

$$R_{rec}(\tau) = \mathfrak{F} R_{uu}(\tau) \tag{15}$$

By inverting the matrix $\mathfrak{F}$, a *corrected* or *refined* estimate of $\hat{R}_{rec}$ can be obtaind

$$\hat{R}^*_{rec}(\tau) = \mathfrak{F}^{-1} \hat{R}_{rec}(\tau) \tag{16}$$

which is now a non-biased and consistent estimator of $R_{uu}(\tau)$. This is illustrated in Fig. 4 for the previous example, in which the PSD deduced from $\hat{R}^*_{rec}(\tau)$ is compared with the input spectrum (an AR2 process: $\phi_1 = 1.5$, $\phi_2 = -0.75$). The improvement in the spectral estimate is dramatic, at least at the lower frequencies.

3. SIMULATION TECHNIQUES AND DESCRIPTION OF THE EXPERIMENT

Both simulations and experiments have been used to investigate the performance of the refined PSD estimate, as illustrated in Fig. 5.

The simulations were based on signal generation as described by Fuchs et al. (1994). Typically a 1st or 2nd order autoregressive process is used to generate a time series, after which particle arrivals are simulated using a refined conveyer-belt model. Thus, all statistics of the underlying process are known, including the PSD, however the data is available as would be measured by an LDA, albeit without noise. The reliability of these simulations has been thoroughly investigated previously [6,7]. These simulations are used to investigate the performance of the estimators as a function of all system parameters,

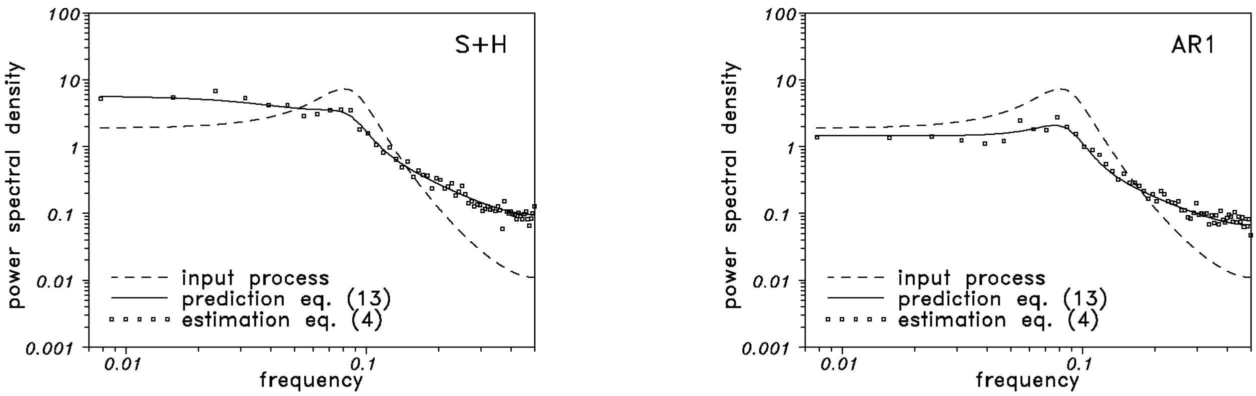

Figure 3: Power spectral density of input process, according to Eq. (13) and according to Eq. (4): a) S+H reconstruction, b) AR1 reconstruction.

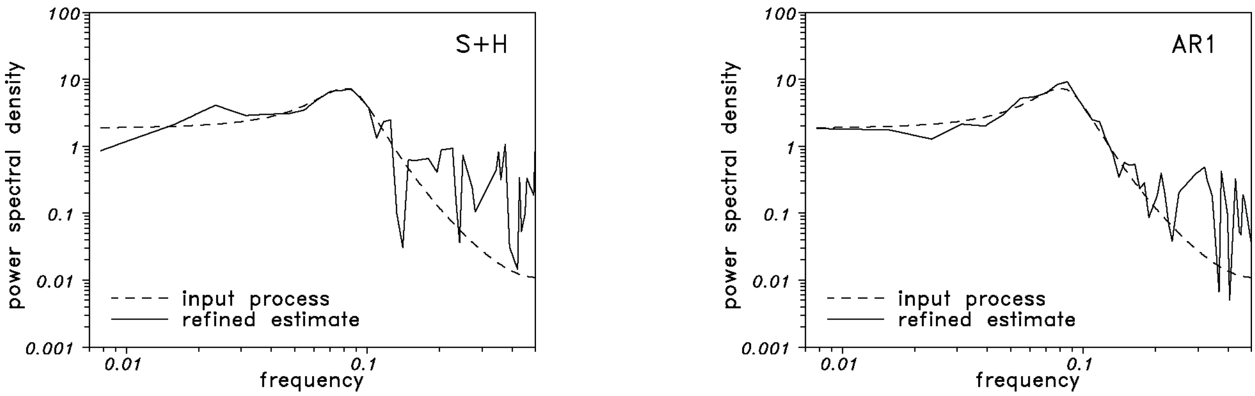

Figure 4: Power spectral density of input process and refined estimate: a) S+H reconstruction, b) AR1 reconstruction.

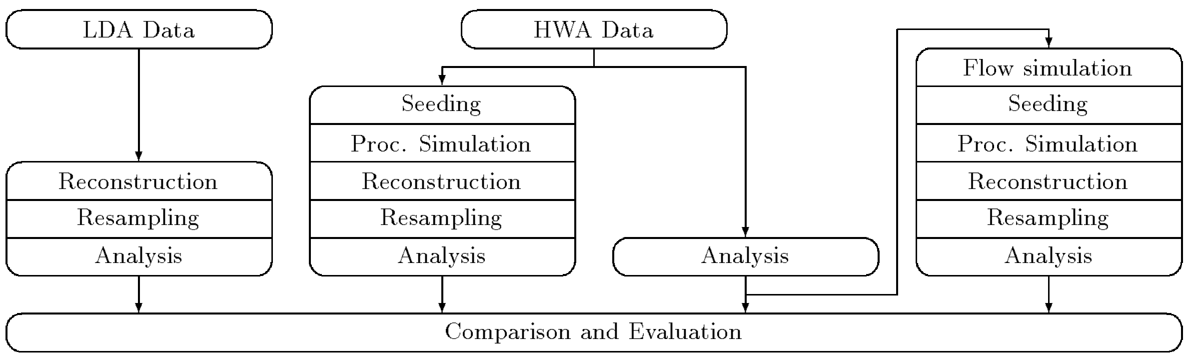

Figure 5: Use of simulations and experiments to evaluate estimator performance

Table 2: Flow specifications

z/D	x/D	Re	$I/(ms)$	$Tu/(\%)$
6	3	40 000	2	24
Re - based on jet outlet diameter and velocity				

Table 3: LDA specifications

Optics	
Power	$10\,mW$
Wavelength	$632.8\,nm$
Mode	forward scatter
MV diameter	$70\,\mu m$
MV length	$470\,\mu m$
Shift	$5\,MHz$
Processor	
Model	Counter TSI 1980
Min. Fringes	16
Mode	Total Burst

including data density (particles/integral time scale), turbulence level, etc. The simulation can be extended by adding white noise to the individual velocity samples, designed to mimic various noise sources present in the LDA system (van Maanen, Tulleken; 1994).

Alternatively, the simulation can use an analog signal sampled at a high rate as an input series. In the present case a hot-wire signal was sampled at $20\,000\,Hz$ for this purpose. The statistics of this signal can still be known within the certainty of the noise in the analog signal.

LDA and hot-wire measurements were performed in an axisymmetric free jet. The integral time scale (I) and turbulence level (Tu) could be selected according to the measurement position as summarized in Table 2. The data density of LDA measurements (N_D number of data samples per integral time scale) was varied either through the seed rate or through signal amplification.

A counter processor (TSI 1980) interfaced (DOSTEK 1400A) to a PC computer was used to process the LDA signals. Specifications of the LDA system are summarized in Table 3. The particle seeding was turned off while HWA measurements were performed at the same measurement position and flow conditions. A DANTEC 55M01 anemometer with a 55P01 single wire probe was used. The signal was filtered at $10\,kHz$ and sampled at $20\,kHz$. The HWA signal was used to determine the integral time scale of the flow fluctuations and also as a reference PSD function.

4. EVALUATION OF THE ESTIMATOR

In the following evaluation only the S+H reconstruction will be examined, since preliminary investigations revealed little difference in comparison to other one-point reconstruction techniques.

The first set of results are presented in Fig. 6 in which the LDA spectral estimate with and without refinement is compared to the HWA spectra for four cases. These cases correspond to the conditions a) high data density ($N_D = 14$); b) high data density but also high noise level ($N_D = 16$); c) and d) low data density ($N_D = 0.63$), short and long data sets respectively.

Examining, first the spectral estimate at a high data density (Fig. 6a), it is apparent that the S+H reconstruction estimate is not capable of resolving the second slope in the spectrum indicated by the HWA data. The second slope in the spectrum is associated with dissipative scales of turbulence. The first slope is termed the inertial subrange. The refinement does not improve the estimate noticeably. The S+H estimate appears smoother at high frequencies than the refined estimate. The S+H yields a systematic error which in this case dominates the random error (noise) in the LDA data set. The refined estimate in fact recovers a portion of this random error, which appears to lead to a larger variance of the estimate, but is probably more realistic of the true spectral content.

The increased noise level of case 2 (Fig. 6b) is apparent both in the raw and the refined spectral estimate, whereby the refined estimate shows a marginal advantage in the range $200\,Hz < f < 500\,Hz$.

The refined estimate shows a distinct advantage, especially at the low data rate of $314\,Hz$ (Fig. 6c and d). The S+H estimate exhibits a low-pass filter behaviour with a cutoff frequency of $314/2\pi \approx 50\,Hz$, whereas the refined estimate appears reliable up to about $1\,000\,Hz$ (Fig. 6d).

Comparing Figs. 6c and d allows the influence of the record length to be evaluated, specifically the estimator variance, which will decrease with increasing record length. The estimation in Fig. 6c extends reliably only to about $500\,Hz$, whereas in Fig. 6d this limit is increased by factor of 2. Correspondingly, the noise level at high frequency also decreases.

The interpretation of the spectrum in Fig. 6d is hindered somewhat because the actual noise level existing in the LDA signal is not known beforehand. To circumvent this difficulty the HWA signal, which clearly has a much lower noise level, was used as the primary input signal for an LDA signal simulation. A high ($N_D = 14$) and low ($N_D = 0.63$) data density was simulated with the respective spectra estimates shown in Fig. 7.

Fig. 7a shows clearly that the refined estimate is very successful in capturing even a portion of the dissipation range of the spectra whereas the raw estimate is filter dominated above $1\,kHz$. The approximate agreement with the true spectrum is only fortuitous in the case of the raw estimate, a situation which has often been misinterpreted in the past. These results indicate that the noise level in Fig. 6a was indeed preventing resolution of the refined spectral estimator.

The same simulation procedure at the low data rate (Fig. 7b) results in estimates in astounding agreement with the original LDA data (Fig. 6c). This is because a rather short data record has been used, in which case the estimator variance is again dominating the estimate at high frequencies.

5. CONCLUSIONS

A new spectral estimator has been introduced which builds on conventional one-point reconstruction estimators and refines these using knowledge about the particle arrival statistics. The above results on a selected number of data sets appear to be at most a modest improvement of LDA spectral estimation. On the other hand a very

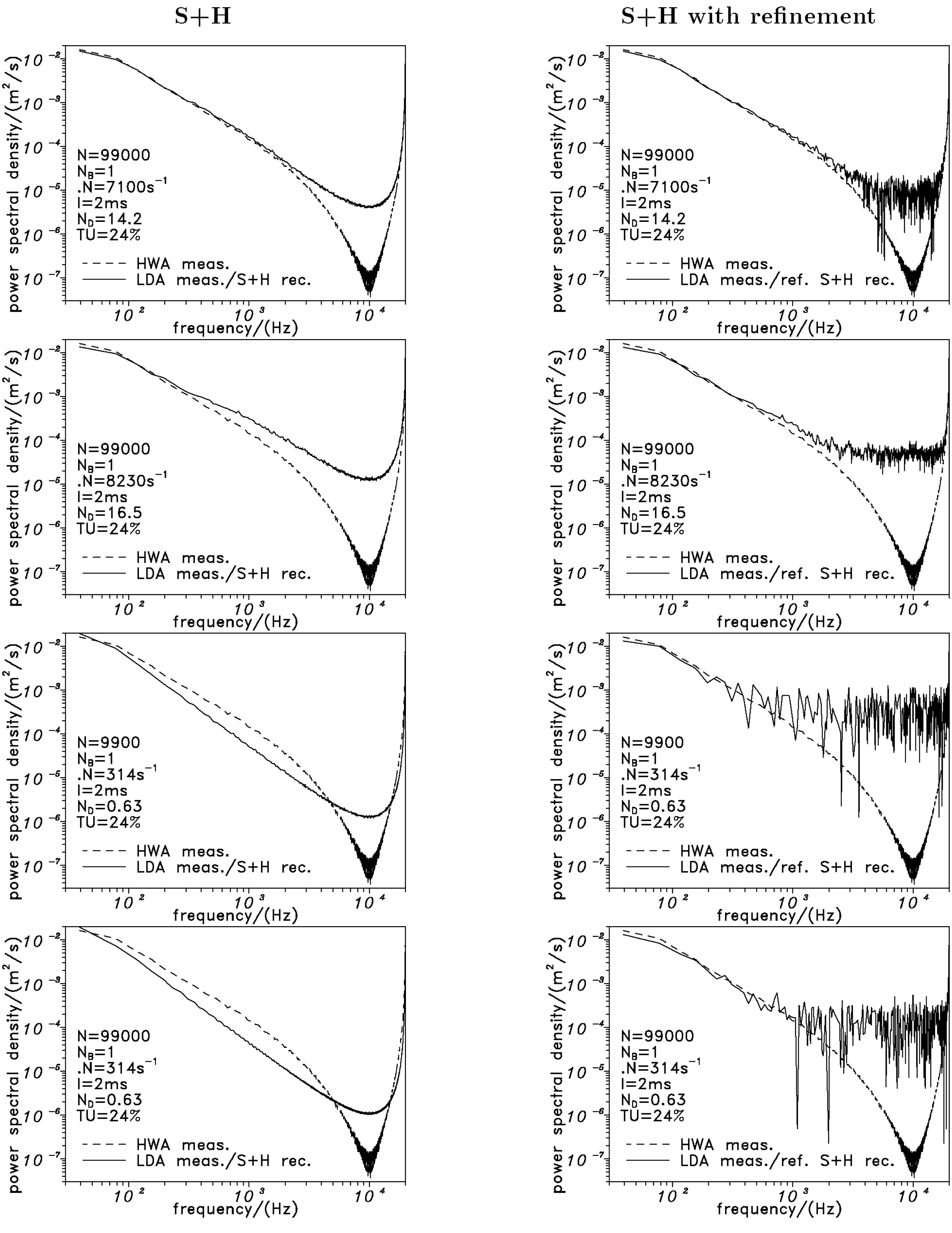

Figure 6: Raw and refined spectra estimates (S+H) compared to HWA spectrum, $Re = 40\,000$: a) $N_D = 14$; b) $N_D = 16$, high noise level; c) $N_D = 0.63$ short data set; d) $N_D = 0.63$ long data set

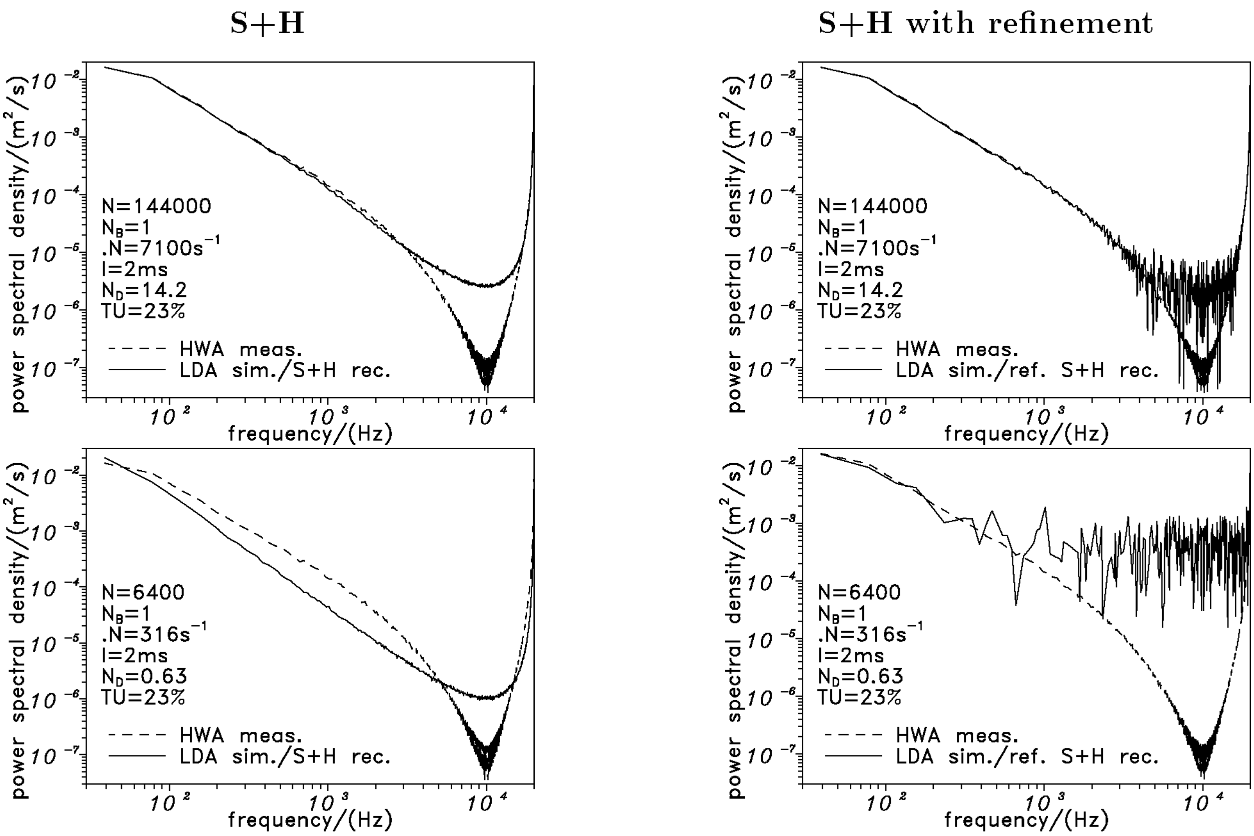

Figure 7: Spectral estimates from simulated LDA data using HWA data as primary input series: a) high data rate b) low data rate

basic feature of reconstruction techniques in general has been overcome, namely the low-pass filter associated with the mean particle rate. It is therefore not surprising that the merits of this new approach become especially apparent at low data rates.

Nevertheless, the presence of noise in the data set will ultimately determine the resolution of the estimator at high frequencies and the remarks concerning the minimizing of these noise sources given in van Maanen and Tulleken (1994) can only be reiterated. In the case of very low noise levels however, all other reconstruction techniques, including the Kalman filter will suffer from filter dominated estimates at low data rates. This is the major advantage of the new, refined estimator.

6. ACKNOWLEDGEMENTS

This work has been carried out with the financial support of the Deutsche Forschungsgemeinschaft under grants Tr 194/9 and Mu 1117/1. Also the help of Mr. T. Unger in taking the hot-wire and LDA measurements at LSTM is acknowledged.

REFERENCES

[1] Adrian, R.J. & Yao, C.S. 1987, Power Spectra of Fluid Velocities Measured by Laser Doppler Velocimetry, *Exp. in Fluids*, vol. 5, pp. 17–28.

[2] Benedict, L.H. & Gould, R.D. 1995, Experiences Using Kalman Reconstruction for Enhanced Power Spectrum Estimates, *Proc. 6th Int. Conf. on Laser Anemometry, Hilton Head.*

[3] Clark, J.J., Palmer, M.R. & Lawrence, P.D. 1985, A Transformation Method for the Reconstruction of Functions from Nonuniformly Spaced Samples, *IEEE Trans. of Acoustics, Speech, and Signal Processing*, vol. ASSP-33, No. 4, pp. 1151-1165.

[4] Edwards, R.V. & Jensen, A.S. 1983, Particle-Sampling Statistics in Laser Anemometers: Sample-and-Hold Systems and Saturable System, *Journal of Fluid Mechanics*, vol. 133, pp. 397–411.

[5] Erdmann, J.C. & Tropea, C. 1982, Statistical Bias of the Velocity Distribution Function in Laser Anemometry, *Proc. 7th Int. Symp. on Appl. of Laser Techn. to Fluid Mechanics, LADOAN, Lisbon*, paper 16.2.

[6] Fuchs, W., Albrecht, H., Nobach, H., Tropea, C. & Graham, L.J.W. 1992, Simulation and Experimental Verification of Statistical Bias in Laser-Doppler Anemometry Including Non-Homogeneous Particle Density, *Proc. 6th Int. Symp. on Appl. of Laser Techn. to Fluid Mechanics, LADOAN, Lisbon.*

[7] Fuchs, W., Nobach, H. & Tropea, C. 1993, The Simulation of LDA Data and its Use to Investigate the Accuracy of Statistical Estimators, *AIAA Journal*, vol. 32, pp. 1883–1889.

[8] Gaster, M. & Roberts, J.B. 1975, Spectral Analysis of Randomly Sampled Signals, *J. Inst. Maths Applics*, vol. 15, pp. 195–216.

[9] Høst-Madsen, A. 1994, A New Method for Estimating Turbulence Spectra for Laser Doppler Anemometry, *Proc. 7th Int. Symp. on Appl. of Laser Techn. to Fluid Mechanics, LADOAN, Lisbon*, paper 11.1.

[10] Lee, D.H. & Sung, H.J. 1992, Turbulent Spectral Bias of Individual Realization of LDV, *Proc. 7th Int. Symp. on Appl. of Laser Techn. to Fluid Mechanics, LADOAN, Lisbon.*

[11] Mayo, W.T. Jr. 1975, Modelling of Laser Velocimeter Signals as Triply Stochastic Poisson Process, *Proc. of Minnesota Symp. on Laser Doppler Anemometry, Bloomington.*

[12] Müller, E., Nobach, H. & Tropea, C. 1994, LDA Signal Reconstruction: Application to Moment and Spectral Estimation, *Proc. 7th Int. Symp. on Appl. of Laser Techn. to Fluid Mechanics, LADOAN, Lisbon*, paper 23.2.

[13] Müller, E., Nobach, H. & Tropea, C. 1995, Model Parameter Estimation from LDA Data at Low Particle Densities, *Proc. 6th Int. Conf. on Laser Anemometry, Hilton Head.*

[14] Roberts, J.B. & Ajmani, D.B.S. 1986, Spectral Analysis of Randomly Sampled Signals Using a Correlation-Based Slotting Technique, *IEEE Proceedings*, vol. 133, Pt. F, No. 2, pp. 153–162.

[15] Roberts, J.B., Downie, J. & Gaster, M. 1980, Spectral Analysis of Signals from a Laser Doppler Anemometer Operating in the Burst Mode, *J. Phys. E: Sci. Instrum.*, vol. 13, pp. 977–981.

[16] Strahle, W.C. 1991, Turbulent Combustion Data Analysis Using Fractals, *AIAA Journal*, vol. 29, No. 3, pp. 409–417.

[17] Tropea, C. 1987, Turbulence-Induced Spectral Bias in Laser Anemometry, *AIAA Journal*, vol. 25, pp. 306–309.

[18] van Maanen, H. & Tulleken, H. 1994, Application of Kalman Reconstruction to Laser-Doppler Anemometry Data for Estimation of Turbulent Velocity Fluctuations, *Proc. 7th Int. Symp. on Appl. of Laser Techn. to Fluid Mechanics, LADOAN, Lisbon*, paper 23.1.

[19] Veynante, D. & Candel, S.M. 1988, A Promising Approach in Laser Doppler Velocimetry Data Processing: Signal Reconstruction and Nonlinear Spectral Analysis, *Signal Processing*, vol. 14, pp. 295–300.